

# Impact of Interfacial Proton Accumulation on Protonation in a Brownmillerite Oxide

Lingling Xie, Yosuke Isoda, Shuri Nakamizo, Takuya Majima, Saburo Hosokawa, Kiyofumi Nitta, Yuichi Shimakawa, and Daisuke Kan\*

Electrochemical protonation provides ways to control physical properties and even explore unprecedented phases of solid-state materials. While how proton accumulation changes materials' properties is investigated, how protonation of solids can be controlled and promoted remains an enigmatic puzzle. In the work reported here, the influence of electrochemical proton injection duration ( $t_{\text{vg}}$ ) is investigated on the protonation of SrCoO<sub>2.5</sub> (SCO) films in electric-field-effect transistor structures with gate layers of the proton-conducting electrolyte Nafion. The proton concentration accumulated in SCO films varies depending on the duration of the proton injection. When protons are injected in a relatively short  $t_{\text{vg}}$  ( $\leq 600$  s), the hydrogen concentration accumulated in SCO film increases with increasing  $t_{\text{vg}}$ , reaching the maximum proton concentration of  $\approx 1.9$  per formula unit of SCO for the  $t_{\text{vg}} = 600$  s case. On the other hand, when  $t_{\text{vg}}$  is longer than 900 s, the proton concentration decreases with  $t_{\text{vg}}$ , implying the occurrence of counterreactions that extract protons from protonated SCO and oxidize the channel. These observations indicate that protons accumulated at the Nafion/SCO interface play a role in the protonation of SCO films and that suppressing the interfacial proton accumulation is the key to maximizing the proton concentration accumulated in SCO films.

## 1. Introduction

Protonation or incorporating protons into transition metal oxides (TMOs), which modulate valence states of transition metals through electron donation associated with the proton incorporation, is a powerful strategy for exploring functional properties and novel phases not seen in original (non-protonated) TMOs.<sup>[1–9]</sup> Various reaction routes for protonating TMOs, such as hydrogen spillover and chemical reduction reactions with metal hydrides, have recently been developed.<sup>[10–12]</sup> Among them, electrochemical hydrogen (proton) injection is a unique approach, for instance, which allows inserting and extracting protons from TMOs at room temperature and controlling TMOs' physical properties in reversible manners.<sup>[13,14]</sup> Electric-field-effect transistor structures with gate layers of electrolytes containing water molecules and protons have been utilized to induce electrochemical insertion and extraction of protons from TMO channel layers by applying gate voltages at room

temperature. The brownmillerite-structured strontium cobaltite SrCoO<sub>2.5</sub> (SCO, orthorhombic  $a = 5.67\text{\AA}$ ,  $b = 5.53\text{\AA}$ , and  $c = 15.59\text{\AA}$  in bulk)<sup>[15]</sup> has an ordered arrangement of oxygen vacancies and is electrochemically reduced by applying gate voltages and injecting protons from H<sub>2</sub>O-containing electrolyte gate layers,<sup>[16,17]</sup> such as ionic liquids containing H<sub>2</sub>O impurities in transistor structures. The oxide can accommodate protons without forming oxygen vacancies ( $\text{SrCoO}_{2.5} + x/2 \text{H}_2 \rightarrow \text{H}_x\text{SrCoO}_{2.5}$ ), and the protonated SCO ( $\text{H}_x\text{SrCoO}_{2.5}$ , referred to as H-SCO) exhibits physical properties depending on proton concentrations.<sup>[18–20]</sup> Although proton accumulation and protonation of SCO have been established, how protons injected from electrolyte layers diffuse into SCO channels remains elusive. Given that regardless of the types of electrolytes (liquids or solids), protons in electrolytes are much more mobile than those in SCO lattices, the proton concentration at the electrolyte/SCO interface would vary depending on both the magnitude of applied gate voltage and the duration of voltage application, implying that protons accumulated at the electrolyte/SCO interface significantly influence protonation and proton evolution in SCO films.

L. Xie, Y. Isoda, Y. Shimakawa, D. Kan  
Institute for Chemical Research  
Kyoto University  
Uji, Kyoto 611-0011, Japan  
E-mail: [dkan@scl.kyoto-u.ac.jp](mailto:dkan@scl.kyoto-u.ac.jp)

S. Nakamizo, T. Majima  
Department of Nuclear Engineering  
Kyoto University  
Kyoto 615-8540, Japan

S. Hosokawa  
Faculty of Materials Science and Engineering  
Kyoto Institute of Technology  
Kyoto 606-8585, Japan

K. Nitta  
Japan Synchrotron Radiation Research Institute  
SPring-8, Sayo, Hyogo 679-5198, Japan

The ORCID identification number(s) for the author(s) of this article can be found under <https://doi.org/10.1002/adfm.202410084>

© 2024 The Author(s). Advanced Functional Materials published by Wiley-VCH GmbH. This is an open access article under the terms of the [Creative Commons Attribution](https://creativecommons.org/licenses/by/4.0/) License, which permits use, distribution and reproduction in any medium, provided the original work is properly cited.

DOI: 10.1002/adfm.202410084

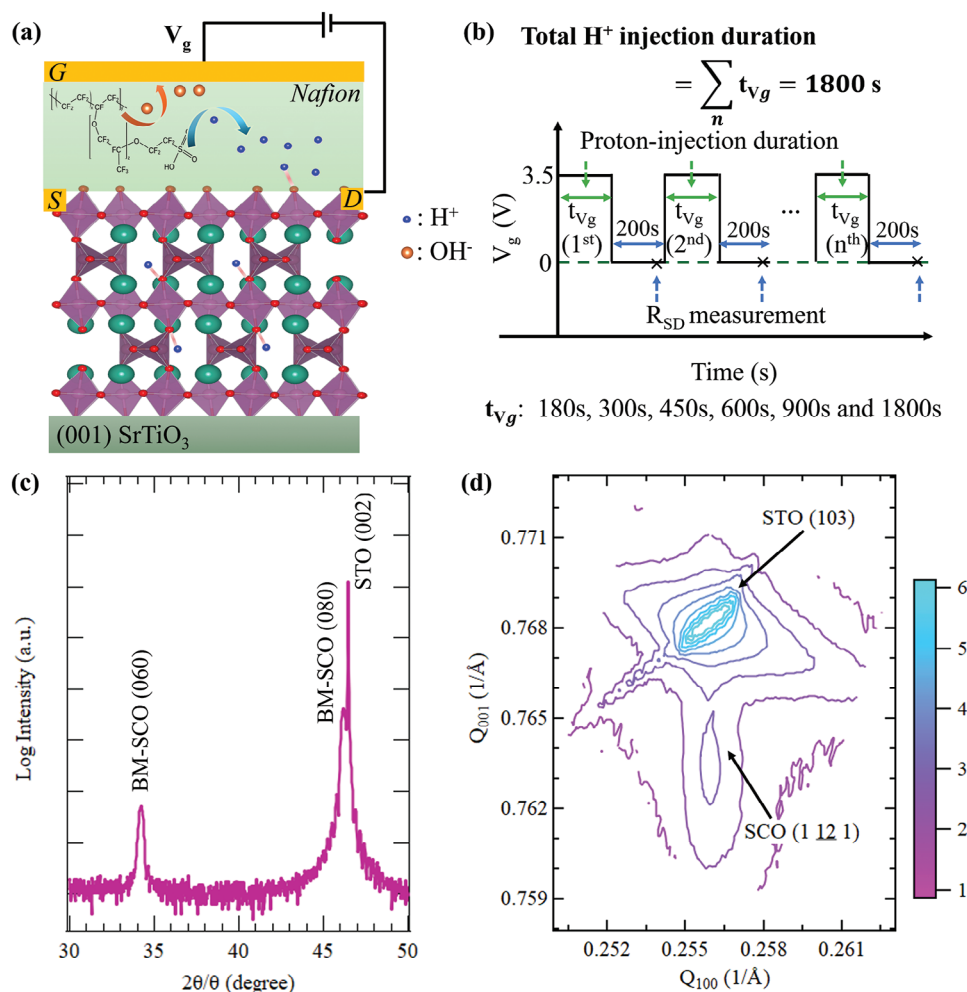


**Figure 1.** a) Schematic of electric-field-effect transistor structures with gate layers of proton-conducting Nafion membranes, which are utilized for inserting protons into SrCoO<sub>2.5</sub> (SCO) film channels by applying positive gate voltages. b) Gate voltage sequence with various proton injection durations  $t_{vg}$ . c) X-ray  $2\theta/\theta$  diffraction profile for 35-nm-thick as-grown SCO films grown on STO substrates. d) Reciprocal space mapping around the (103) SrTiO<sub>3</sub> reflection for 35-nm-thick as-grown SCO film. The diffraction intensity is plotted on the logarithmic scale.

Previously, we showed that a proton-conducting solid-state electrolyte (Nafion membranes) can be utilized as a gate layer in transistor structures for electrochemically injecting protons into oxygen-deficient perovskite oxides such as SrFeO<sub>x</sub> epitaxial films. Electrochemically inserting and extracting protons by applying gate voltages through Nafion layers at room temperature was shown to allow for controlling structural and transport properties of SrFeO<sub>x</sub> in reversible and non-volatile manners, demonstrating the usefulness of the proton-conducting solid-state electrolyte for protonating oxides.<sup>[8,9]</sup> However, how proton evolution induced by proton injection can be controlled and how the proton accumulation in oxides can be maximized remains elusive. In this study, we adopted Nafion membranes ( $\approx 127 \mu\text{m}$  thick) as gate layers in transistor structures with channels of the brownmillerite-structured SrCoO<sub>2.5</sub>, as schematically shown in **Figure 1a**, and investigated the influence of durations of proton injections (or durations of gate voltage application) on the proton accumulation in SCO epitaxial films. Proton diffusion and accumulation in SCO films are driven by the chemical potential difference of protons

within and outside the oxide. If the chemical potential outside is higher than the potential inside SCO, protons will be diffused toward the oxide. When the proton injection duration ( $t_{vg}$ ) is longer and the chemical potential difference becomes smaller, protons injected into SCO films under positive gate voltages would begin to accumulate at the interface, and their concentration would be larger. Given that protons in Nafion are rather mobile than those in the SCO lattice, the mobility difference at the Nafion/SCO interface further results in the interfacial proton accumulation. Importantly, when the gate voltage is turned off, the field-induced gradient of proton distribution within Nafion layers will return to equilibrium, and consequently, the interfacial proton accumulation will be relaxed while the protons accumulated in SCO films remain because the chemical potential reaches equilibrium.

We show that when the protons are injected for various durations and the total time of proton injection is fixed, as shown in **Figure 1b**, the proton concentration accumulated in SCO ( $x_H$ ) varies depending on the proton injection duration ( $t_{vg}$ ). For voltage sequences with  $t_{vg}$  up to 600 s, the hydrogen

concentration accumulated in SCO film increases with increasing  $t_{\text{vg}}$  and reaches the maximum  $x_{\text{H}} \approx 1.9$  (per formula unit of SCO) when  $t_{\text{vg}} = 600$  s. On the other hand, when protons are injected in voltage sequences with  $t_{\text{vg}}$  longer than 900 s,  $x_{\text{H}}$  is found to be largely reduced from the maximum value, implying the occurrence of counterreactions that oxidize the channel and extract hydrogen from protonated SCO. Based on our experimental results, we discuss the protonation process in SCO films, focusing on the significance of protons accumulated at the Nafion/SCO interface.

## 2. Results and Discussion

Brownmillerite-structured  $\text{SrCoO}_{2.5}$  (SCO) films were grown on  $\text{TiO}_2$ -terminated (001)  $\text{SrTiO}_3$  (STO) substrates by pulsed laser deposition. Figure 1c,d shows the X-ray  $2\theta/\theta$  diffraction profile around the (002) STO reflection and reciprocal space mapping (RSM) around the (103) STO reflection. In the  $2\theta/\theta$  diffraction profile, a reflection from the SCO film seen at  $2\theta \approx 46.5^\circ$  can be indexed as (080) of the brownmillerite structure. The films' superstructure reflection seen at  $2\theta \approx 34.2^\circ$  (and  $2\theta \approx 58.7^\circ$  in Figure S1, Supporting Information), which can be indexed as (060) (and (0 10 0)), can be regarded as a consequence of the periodic stacking of layers of the  $\text{CoO}_4$  oxygen tetrahedra and  $\text{CoO}_6$  oxygen octahedra along the out-of-plane direction, characteristic of the brownmillerite structure. Furthermore, as seen in RSM (Figure 1b), the (1 12 1) SCO reflection appears at the same position along the in-plane direction as the (103) STO reflection, indicating the lattice matching between the SCO and STO lattices whose in-plane epitaxial relationship is  $[101]_{\text{SCO}} // [100]_{\text{STO}}$ . These observations indicate the epitaxial growth of the brownmillerite-structured SCO with the (010) orientation on (001) STO substrates.

To protonate SCO films and investigate the influence of proton injection duration on their proton accumulation, we fabricated electric-field-effect transistor structures whose channels are SCO films and gate layers are Nafion membranes. We applied sequences of the gate voltage of + 3.5 V for various durations (referred to as  $t_{\text{vg}}$ , ranging from 180 to 1800 s) and electrochemically injected protons into SCO channels. As shown in Figure 1b, the total time for the proton injection was fixed to be 1800 s. At the interval between gate voltage pulses, the gate voltage was turned off for 200 s, and the SCO channels' electrical resistance was measured under the source-drain voltage of 0.1 V. Figure 2a shows changes in the resistance of SCO channels during proton injection with the voltage pulse sequence with  $t_{\text{vg}} = 180, 300, 450, 600, 900,$  and 1800 s. The resistance plotted in the figure was normalized by the resistance of the as-grown state ( $R_0$ ). For all voltage sequences, the protons were injected for a total of 1800 s. The proton-injection-induced resistance change is found to depend on  $t_{\text{vg}}$ . For the cases with  $t_{\text{vg}}$  shorter than 450 s, the resistance increases slightly with proton injection, and the resistance remains as low as  $R/R_0 \approx 3$  after the proton injection. With further increasing  $t_{\text{vg}}$ , the proton injection leads to large resistance increases, and the resistance after the proton injection reaches up to  $R/R_0 \approx 50$ . Nonetheless, when  $t_{\text{vg}}$  is increased up to 1800 s, the resistance after proton injection remains comparable to that of the as-grown state ( $R_0$ ). The observed  $t_{\text{vg}}$  dependence on the resistance changes implies that proton injection by the voltage pulse sequence with relatively short  $t_{\text{vg}}$  leads to protonation of

SCO channels. Consequently, the Co valence states are modulated through the protonation-induced electron donation. On the other hand, the voltage sequence with longer  $t_{\text{vg}}$  results in the additional occurrence of a reaction process that counteracts the protonation of the SCO channels.

To further shed light on the  $t_{\text{vg}}$ -dependent protonation process, we characterized the structural phases of SCO films after proton injection for a total of 1800 s and evaluated their proton concentration. These measurements were performed for the films whose surfaces were exposed by peeling off Nafion membranes after electrochemical protonation. Figure 2b,c, respectively, shows the X-ray  $2\theta/\theta$  diffraction patterns and the elastic recoil detection analysis (ERDA) spectra for SCO films after proton injection by the voltage sequence with  $t_{\text{vg}} = 180, 300, 450, 600, 900,$  and 1800 s. We note that the X-ray diffraction patterns of SCO films remained almost unchanged when Nafion membranes were simply pressed and peeled off (without gate voltage application), as shown in Figure S2 (Supporting Information). The (080) reflection of the SCO films proton-injected with the  $t_{\text{vg}} = 180$  s sequence is seen at almost the same position as the one for the as-grown film, implying that few or no injected protons are accumulated in SCO films. Given that protonated SCO epitaxial films (H-SCO) were shown to have a larger out-of-plane lattice constant than that for the (010)-oriented SCO films, the appearance of the reflection at  $2\theta \approx 44.3^\circ$  for films proton-injected with the  $t_{\text{vg}} = 300, 450,$  and 600 s sequences and the concomitant changes in the (060) reflection (Figure S3, Supporting Information) indicate that the injected protons are accumulated in the SCO lattices.<sup>[18]</sup> We also confirmed that no changes in the structure and resistance of the SCO films were seen after applying the  $t_{\text{vg}} = 600$  s voltage sequence directly to SCO channels without the Nafion gate layer (Figure S4, Supporting Information). Our results indicate that the electric field drop across the SCO film is different between the interfaces with and without the Nafion gate layer, highlighting that the Nafion gate layer and its interface play significant roles in protonation processes in SCO films.

In the ERDA spectra, the recoiled H atoms from these films are observed as a broad peak, which can be well reproduced by assuming two contributions: one by H adsorbed on the SCO surfaces ( $\approx 1050$  keV), and the other by H recoiled forward from the bulk film region ( $\approx 950$  keV, referred to as the bulk H).<sup>[8]</sup> We note that the peak originating from the bulk H increases with increasing  $t_{\text{vg}}$ , highlighting the significance of  $t_{\text{vg}}$  for the proton accumulation in SCO films. These observations indicate that protonation in SCO films proceeds along the out-of-plane direction that is parallel to the direction of the periodic stacking of the  $\text{CoO}_6$  and  $\text{CoO}_4$  layers, although proton migration and diffusion through the  $\text{CoO}_4$  tetrahedral layers are theoretically suggested to be unfavorable.<sup>[21]</sup> Further investigations will be needed to clarify the proton migration and diffusion on the atomic level.

Importantly, ERDA signals from the bulk H contribution are found to be heavily reduced for the films proton-injected with the  $t_{\text{vg}} = 900$  and 1800 s sequences. While these films exhibit the reflections from H-SCO, their reflection intensities are apparently weak, particularly for the film protonated with the  $t_{\text{vg}} = 1800$  s sequence. (Figure 2b; Figure S3, Supporting Information). It should also be pointed out that for the  $t_{\text{vg}} = 1800$  s case, in addition to the H-SCO reflection, the small reflection at  $2\theta \approx 47.6^\circ$ , which can be indexed as (002) for the perovskite structure, is

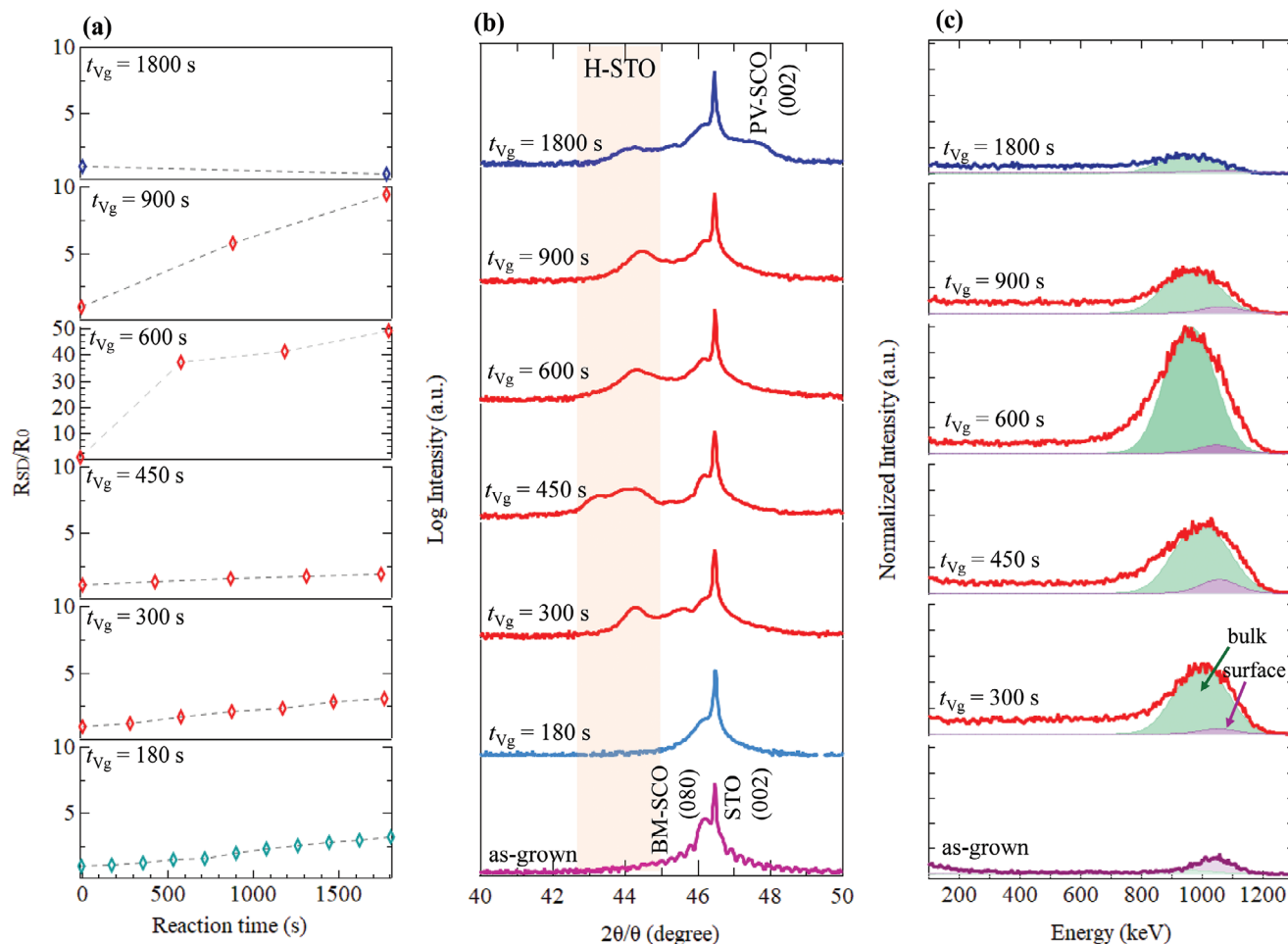


**Figure 2.** a) Changes in the resistance of SrCoO<sub>2.5</sub> (SCO) channels during proton injection with the voltage pulse sequences with the duration  $t_{Vg} = 180, 300, 450, 600, 900,$  and  $1800$  s. The resistance plotted in the figure was normalized by that of the as-grown films. b) X-ray  $2\theta/\theta$  diffraction patterns around the (002) STO reflections for SCO films after proton injection by the voltage sequences with  $t_{Vg} = 180, 300, 450, 600, 900,$  and  $1800$  s. c) Elastic recoil detection analysis (ERDA) spectra for as-grown SCO film and after proton injection by the voltage sequences with  $t_{Vg} = 300, 450, 600, 900,$  and  $1800$  s. The spectrum for the as-grown film was taken after simply pressing a Nafion membrane for 1 h and peeling it off without gate voltage application. The contributions of the H atoms recoiled forward from the bulk film region (the bulk H contribution), which was determined by fitting the spectra, were also shown.

seen. We also note that the resistivity of the film protonated with the  $t_{Vg} = 1800$  s sequence is lower than the resistivities of as-grown film and the film protonated with the  $t_{Vg} = 600$  s sequence (Figure S5, Supporting Information). Taking into consideration that the perovskite phase of SrCoO<sub>2.5+ $\delta$</sub>  with electrical conduction should be formed by oxidizing the brownmillerite phase of SrCoO<sub>2.5</sub>,<sup>[19,22–25]</sup> the reduction in the accumulated protons for the 900 and 1800 s sequences can be understood to result from the occurrence of counterreaction that extracts hydrogen from the protonated SCO film and oxidizes the films. This can also explain why the film proton-injected with the  $t_{Vg} = 1800$  s sequence has low resistance, comparable to that of the as-grown state (Figure 2a).

Figure 3a shows the  $t_{Vg}$  dependence of the proton concentration accumulated in SCO films, determined from the bulk H contribution in the ERDA signals and by the assumption that protons are distributed homogeneously in the films' entire regions. Increasing  $t_{Vg}$  up to 600 s increases the proton concen-

tration and reaches the maximum  $x_H \approx 1.9$  (per formula unit of SCO). This proton concentration is much larger than that expected from the Co valence change from 3+ for SrCoO<sub>2.5</sub> to 2+ for the protonated phase. A recent investigation<sup>[26]</sup> showed that neutral H–H dimers could be stored in oxygen vacancy channels in the CoO<sub>4</sub> layers of SCO, allowing proton accumulation up to  $x_H \approx 2$  in SCO. Therefore, both protons and H–H dimers are accumulated in the film protonated with  $t_{Vg} = 600$  s sequence. On the other hand, when protons are injected with the voltage sequences with  $t_{Vg}$  longer than 900 s,  $x_H$  is heavily reduced from the maximum value, resulting from the additional occurrence of the counterreaction that oxidizes the channel and extracts hydrogen from protonated SCO.

X-ray absorption measurements further confirm the occurrence of the counterreaction for the SCO films protonated with the  $t_{Vg} = 600$  and 1800 s sequences. Figure 3b shows XAS spectra around the Co *K*-edge for the as-grown SCO film and the films protonated with the  $t_{Vg} = 600$  and 1800 s sequences. In Co *K*-edge

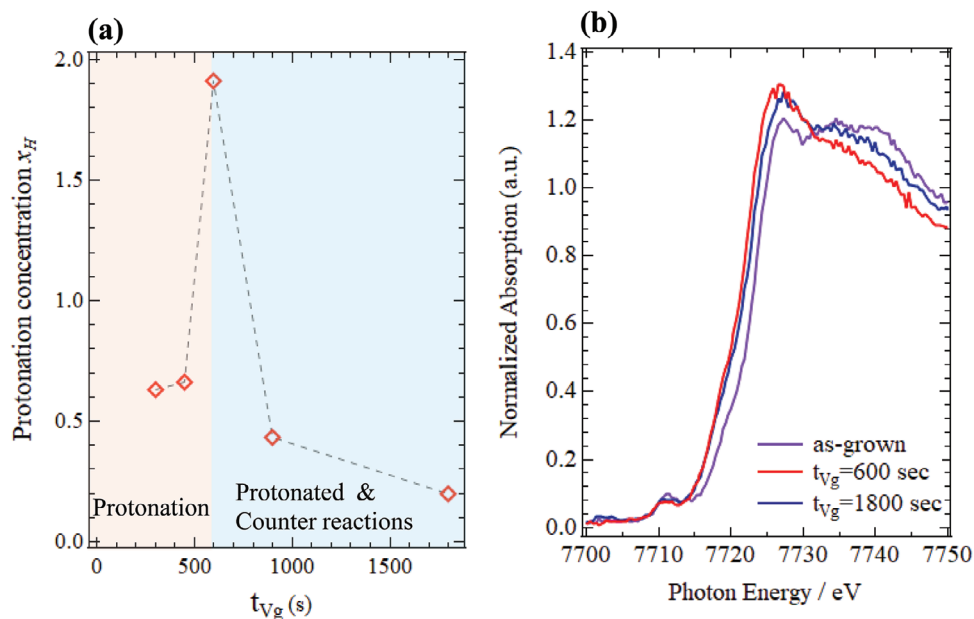


**Figure 3.** a) The duration ( $t_{Vg}$ ) dependence of the proton concentration accumulated in SrCoO<sub>2.5</sub> (SCO) films, determined by the ERDA characterization. b) Normalized X-ray absorption spectra in the energy region around Co K-edge absorptions for as-grown SCO films and the SCO films proton-injected with the  $t_{Vg} = 600$  and 1800 s voltage sequences.

spectra, the absorption edges of the film protonated with the  $t_{Vg} = 600$  s sequence shift toward the lower energy sides from that of the as-grown films, indicating that proton accumulation into SCO films contributes electrons to Co, leading to the lowering of the Co valence state. Notably, the absorption edges of the film protonated with  $t_{Vg} = 1800$  s appear in the energy region higher than that of the film protonated with the  $t_{Vg} = 600$  s sequence and lower than that of the as-grown film. These observations support the occurrence of the counterreaction that suppresses the protonation of the SCO films in the voltage sequence with the long  $t_{Vg}$ .

Finally, we discuss why the protonation of SCO films depends on the proton-injection duration  $t_{Vg}$ . Based on our observations, we propose a mechanism in which protons accumulated at the Nafion/SCO interface play a significant role in the proton evolution and protonation of SCO films, as schematically shown in **Figure 4**. While the chemical potential difference drives proton diffusion and accumulation toward SCO films, the protons in Nafion have much larger mobility than protons in SCO films. Thus, relatively long proton-injection durations are necessary to allow proton evolution in SCO films, and no protonation of SCO films occurs when the  $t_{Vg}$  is relatively short ( $t_{Vg} \leq 180$  s, **Figure 4a**). For the voltage sequences with  $t_{Vg}$  long enough for proton evolution in SCO films ( $300 \text{ s} \leq t_{Vg} \leq 600$  s, **Figure 4b**), the proton concentration accumulated within SCO films increases with the increase in  $t_{Vg}$ , and the proton concentration accumulated at the interface also increases while the chemical potential approaches and reaches equilibrium. When the  $t_{Vg}$  is even longer ( $900 \text{ s} \leq t_{Vg}$ , **Figure 4c**), large amounts of protons are still injected, and the interfacial proton accumulation proceeds because there is almost no chemical potential difference and the proton accumulation into SCO films is limited. It should be noted that protons in Nafion are produced through the water

electrolysis reaction. Thus, simultaneously produced hydroxyls ( $\text{OH}^-$ ) coexist in Nafion, influencing the distribution of these chemical species and even affecting the properties of SCO films, especially when large amounts of protons remain at the Nafion/SCO interface. Since an increase in the interfacial proton accumulation makes the interface regions of SCO films energetically unstable, counterreactions in which hydroxyls ( $\text{OH}^-$ ) left in Nafion react with the protons accumulated at the Nafion/SCO interface should occur and compromise the interfacial energy instability, influencing the proton evolution and protonation of SCO films. As a result of the occurrence of the counterreaction, the protonated SCO films are oxidized, and the protonation of films is suppressed in the voltage sequence with long  $t_{Vg}$ , as confirmed by the observation of the (002) reflection from the perovskite phase of SCO films and the decrease in proton concentration. These considerations imply that the proton injection duration necessary to maximize the proton concentration ( $t_{Vg} = 600$  s for the 35-nm-thick film) should depend on the film thickness and should be shorter for thinner films because the chemical potential for thinner films would reach equilibrium in the voltage sequence with shorter  $t_{Vg}$ . In fact, as shown in **Figure S6** (Supporting Information), the counterreaction for 25-nm-thick SCO films is found to occur in the voltage sequence with  $t_{Vg} = 600$  s, supporting our scenario. We also point out that the counterreaction occurs in transistor structures under positive bias voltages, and the negatively charged  $\text{OH}^-$  (and oxide ions  $\text{O}^{2-}$ ) responsible for the counterreactions are expected not to diffuse less into the film's region. Therefore, the influence of the counterreactions might dominate the film's surface region, and the distribution of the protons within the films would become inhomogeneous. Although we believe that the counterreaction due to interfacial proton accumulation is not limited to only SCO films and could occur with other similar materials if a

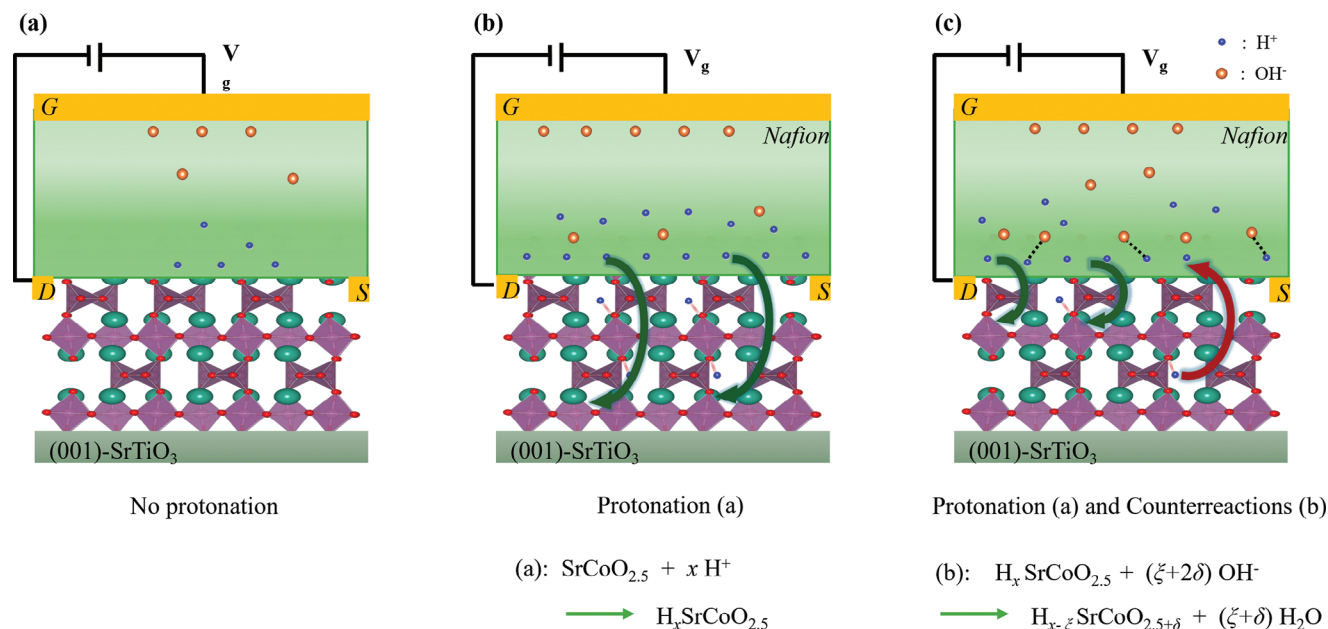


**Figure 4.** Schematics for proton evolution and reactions induced by proton injections with the voltage sequences with a) the duration ( $t_{\text{vg}} \leq 180$  s, b)  $300 \text{ s} \leq t_{\text{vg}} \leq 600$  s, and c)  $900 \text{ s} \leq t_{\text{vg}}$ . In c), counterreactions involving  $\text{OH}^-$  compromise the energy instability due to the interfacial proton accumulation.

large amount of protons accumulate at the interface, further investigation will be necessary for a deeper understanding of electrochemical reactions at the Nafion/SCO interface, including the counterreaction under positive bias voltages and the resultant distribution of the protons within the SCO film and Nafion layer, which would help evaluate how protonation and counterreactions affect the electronic structure (XAS spectra) of SCO films.

### 3. Summary

We show that the proton evolution and protonation of SCO induced by electrochemical proton injection in the transistor structures, consisting of gate layers with proton-conducting Nafion, strongly depend on the proton injection duration ( $t_{\text{vg}}$ ). Furthermore, the  $t_{\text{vg}}$ -dependent protonation can be understood by considering the mechanism in which the proton accumulation at the Nafion/SCO interface plays a significant role in the proton evolution and protonation of SCO films. Our results indicate that adjusting the interfacial proton concentration by controlling the proton-injection duration and suppressing the occurrence of oxidizing reactions that counteract the protonation is the key to promoting proton evolution and maximizing the proton concentration accumulated in SCO films.

### 4. Experimental Section

**Fabrication of Epitaxial Films and Transistor Structures:** 35 nm-thick  $\text{SrCoO}_{2.5}$  (SCO) thin films were epitaxially grown on STO (001) substrates by pulsed laser deposition with a KrF excimer laser ( $\lambda = 248$  nm). SCO films were deposited by ablating ceramic targets with nominal cation compositions with a laser fluence of  $1.1 \text{ J cm}^{-2}$  and at the repetition frequency of 4 Hz. During the film growth, the substrate temperature and oxygen partial pressure were kept at  $700$  °C and 100 mTorr, respectively. After the

deposition, SCO films were cooled to room temperature under the oxygen pressure of 100 mTorr with a cooling rate of  $\approx 20$  °C·min $^{-1}$ .

To protonate SCO films, we fabricated transistor structures whose channels were SCO films and gate layers were proton-conducting electrolytes (Nafion 115, purchased from Chemours Japan) and applied gate voltages through Nafion membranes ( $\approx 127$   $\mu\text{m}$  thick) to electrochemically inject protons into SCO films at room temperature in air condition. 10-nm-thick Pt layers that serve as source and drain electrodes were first sputtered on the SCO films at room temperature. Then, Nafion films with Pt electrodes sputtered on one side were bonded on SCO channels by thermal adhesion at  $110$  °C for 15 min. The voltage sequences for protonating SCO films are shown in Figure 1b. Sequences of the gate voltage of +3.5 V were applied for various durations (ranging from 180 to 1800 s), and protons were injected electrochemically into SCO channels. The total duration for the proton injection was fixed to be 1800 s. At the interval between gate voltage pulses, the gate voltage was turned off for 200 s, and the SCO channels' electrical resistance was measured under the source-drain voltage of 0.1 V.

**Characterization for As-Grown and Protonated SCO Films:** Structural properties of as-grown and protonated SCO films were characterized by X-ray  $2\theta/\theta$  diffraction measurements with a lab-source four-circle diffractometer (X'Pert MRD, PANalytical) using the  $\text{Cu K}\alpha_1$  radiation. The Co K-edge x-ray absorption fine structure (XAFS) spectra were measured at the BL01B1 beamline of the SPring-8. A Si (111) double-crystal monochromator was used to obtain the incident X-ray beam, and the data were collected in fluorescence mode using a 19-element Ge solid state detector. All data were analyzed using the xTunes program, and details about measurements were provided in the previous report.<sup>[27]</sup>

Elastic recoil detection analysis (ERDA) was utilized to quantify the proton concentration accumulated in SCO films. Spectra were obtained for protonated SCO films whose surfaces were exposed by peeling off Nafion membranes after electrochemical protonation. The measurements were conducted at the 1.7 MV tandem accelerator facility of the Quantum Science and Engineering Center, Kyoto University. The spectra were obtained with 7.5 MeV  $\text{Si}^{4+}$  beams incident at an angle  $\sim 45^\circ$  to the surface normal and by collecting H atoms recoiling forward from the films at a scattering angle of  $30^\circ$ . The obtained ERDA spectra were simulated and fitted with the SIMNRA 7.03 software.<sup>[28]</sup>

## Supporting Information

Supporting Information is available from the Wiley Online Library or from the author.

## Acknowledgements

This work was partly supported by Grants-in-Aid for Scientific Research (No. 19H05816, 19H05823, 20H05293, 21H01810, 22H04617, 22H01523, 22KK0075, 23KJ1239, 23H05457, and 24KJ1371) and by grants for the Integrated Research Consortium on Chemical Sciences and the International Collaborative Research Program of the Institute for Chemical Research in Kyoto University from the Ministry of Education, Culture, Sports, Science, and Technology (MEXT) of Japan. The work was also supported by JST SPRING, grant no. JPMJSP2110 and the Japan Science and Technology Agency (JST) as part of the Advanced International Collaborative Research Program (AdCORP), grant no. JPMJKB 2304 and the Adopting Sustainable Partnerships for Innovative Research Ecosystem (ASPIRE) grants no. JPMJAP2312 and JPMJAP2314. The X-ray absorption experiments were performed with the approval of the Japan Synchrotron Radiation Research Institute (Proposal No. 2023B2008).

## Conflict of Interest

The authors declare no conflict of interest.

## Data Availability Statement

The data that support the findings of this study are available from the corresponding author upon reasonable request.

## Keywords

brownmillerite oxide, interfacial proton accumulation, protonation, SrCoO<sub>2.5</sub> epitaxial films

Received: June 10, 2024  
Revised: September 15, 2024  
Published online:

- [1] Y. Guan, H. Han, F. Li, G. Li, S. S. P. Parkin, *Annu. Rev. Mater. Res.* **2023**, *53*, 25.
- [2] C. Leighton, *Nat. Mater.* **2019**, *18*, 13.
- [3] J. Shi, S. D. Ha, Y. Zhou, F. Schoofs, S. Ramanathan, *Nat. Commun.* **2013**, *4*, 2676.
- [4] J. Tian, H. Wu, Z. Fan, Y. Zhang, S. J. Pennycook, D. Zheng, Z. Tan, H. Guo, P. Yu, X. Lu, G. Zhou, X. Gao, J. Liu, *Adv. Mater.* **2019**, *31*, 1903679.
- [5] A. Fluri, E. Gilardi, M. Karlsson, V. Roddatis, M. Bettinelli, I. E. Castelli, T. Lippert, D. Pergolesi, *J. Phys. Chem. C* **2017**, *121*, 21797.
- [6] J. Park, C. Oh, J. Son, *J. Mater. Chem. C* **2021**, *9*, 2521.
- [7] J. Yang, C. Ge, J. Du, H. Huang, M. He, C. Wang, H. Lu, G. Yang, K. Jin, *Adv. Mater.* **2018**, *30*, 1801548.
- [8] Y. Isoda, D. Kan, T. Majima, Y. Shimakawa, *Appl. Phys. Express* **2023**, *16*, 015506.
- [9] Y. Isoda, D. Kan, Y. Ogura, T. Majima, T. Tsuchiya, Y. Shimakawa, *Appl. Phys. Lett.* **2022**, *120*, 091601.
- [10] T. Kamada, T. Ueda, S. Fukuura, T. Yumura, S. Hosokawa, T. Tanaka, D. Kan, Y. Shimakawa, *J. Am. Chem. Soc.* **2023**, *145*, 1631.
- [11] A. Baldi, T. C. Narayan, A. L. Koh, J. A. Dionne, *Nat. Mater.* **2014**, *13*, 1143.
- [12] H. Yoon, M. Choi, T.-W. Lim, H. Kwon, K. Ihm, J. K. Kim, S.-Y. Choi, J. Son, *Nat. Mater.* **2016**, *15*, 1113.
- [13] H. Han, Q. Jacquet, Z. Jiang, F. N. Sayed, J.-C. Jeon, A. Sharma, A. M. Schankler, A. Kakekhani, H. L. Meyerheim, J. Park, S. Y. Nam, K. J. Griffith, L. Simonelli, A. M. Rappe, C. P. Grey, S. S. P. Parkin, *Nat. Mater.* **2023**, *22*, 1128.
- [14] Q. Wang, Y. Gu, C. Chen, L. Han, M. U. Fayaz, F. Pan, C. Song, *ACS Appl. Mater. Interfaces* **2024**, *16*, 3726.
- [15] C. Mitra, T. Meyer, H. N. Lee, F. A. Reboredo, *J. Chem. Phys.* **2024**, *141*, 084710.
- [16] Y. Sun, T. N. H. Nguyen, A. Anderson, X. Cheng, T. E. Gage, J. Lim, Z. Zhang, H. Zhou, F. Rodolakis, Z. Zhang, I. Arslan, S. Ramanathan, H. Lee, A. A. Chubykin, *ACS Appl. Mater. Interfaces* **2020**, *12*, 24564.
- [17] L. Xie, Y. Isoda, T. Majima, Y. Shen, D. Kan, Y. Shimakawa, *J. Solid State Electrochem.* **2023**, <https://link.springer.com/article/10.1007/s10008-023-05759-5>.
- [18] N. Lu, P. Zhang, Q. Zhang, R. Qiao, Q. He, H.-B. Li, Y. Wang, J. Guo, D. Zhang, Z. Duan, Z. Li, M. Wang, S. Yang, M. Yan, E. Arenholz, S. Zhou, W. Yang, L. Gu, C.-W. Nan, J. Wu, Y. Tokura, P. Yu, *Nature* **2017**, *546*, 124.
- [19] Q. Yang, H. J. Cho, H. Jeon, H. Ohta, *Adv. Mater. Interfaces* **2019**, *6*, 1901260.
- [20] N. Lu, Z. Zhang, Y. Wang, H.-B. Li, S. Qiao, B. Zhao, Q. He, S. Lu, C. Li, Y. Wu, M. Zhu, X. Lyu, X. Chen, Z. Li, M. Wang, J. Zhang, S. C. Tsang, J. Guo, S. Yang, J. Zhang, K. Deng, D. Zhang, J. Ma, J. Ren, Y. Wu, J. Zhu, S. Zhou, Y. Tokura, C.-W. Nan, J. Wu, et al., *Nat. Energy* **2022**, *7*, 1208.
- [21] M. S. Islam, A. M. Nolan, S. Wang, Q. Bai, Y. Mo, *Chem. Mater.* **2020**, *32*, 5028.
- [22] H. Jeon, W. S. Choi, J. W. Freeland, H. Ohta, C. U. Jung, H. N. Lee, *Adv. Mater.* **2013**, *25*, 3651.
- [23] H. Jeon, W. S. Choi, M. D. Biegalski, C. M. Folkman, I.-C. Tung, D. D. Fong, J. W. Freeland, D. Shin, H. Ohta, M. F. Chisholm, H. N. Lee, *Nat. Mater.* **2013**, *12*, 1057.
- [24] N. Ichikawa, M. Iwanowska, M. Kawai, C. Calers, W. Paulus, Y. Shimakawa, *Dalton Trans.* **2012**, *41*, 10507.
- [25] S. Lu, F. Yin, Y. Wang, N. Lu, L. Gao, H. Peng, Y. Lyu, Y. Long, J. Li, P. Yu, *Adv. Funct. Mater.* **2023**, *33*, 2210377.
- [26] H. Li, F. Lou, Y. Wang, Y. Zhang, Q. Zhang, D. Wu, Z. Li, M. Wang, T. Huang, Y. Lyu, J. Guo, T. Chen, Y. Wu, E. Arenholz, N. Lu, N. Wang, Q. He, L. Gu, J. Zhu, C. Nan, X. Zhong, H. Xiang, P. Yu, *Adv. Sci.* **2019**, *6*, 1901432.
- [27] H. Asakura, S. Yamazoe, T. Misumi, A. Fujita, T. Tsukuda, T. Tanaka, *Radiat. Phys. Chem.* **2020**, *175*, 108270.
- [28] M. Mayer, SIMNRA User's Guide, Report No. IPP 9/113, Max-Planck-Institut für Plasmaphysik, Garching, Germany **1997**.